ELSEVIER

Journal of Alloys and Compounds 446–447 (2007) 397–401

Journal of ALLOYS AND COMPOUNDS

www.elsevier.com/locate/jallcom

A high-resolution neutron scattering study of the hydrogen-driven metal-insulator phase transition in KC_8H_x

Arthur Lovell [a,*], Neal T. Skipper [a], Steve M. Bennington [b], Ron I. Smith [b]

[a] *Department of Physics and Astronomy, University College London, Gower Street, London WC1E 6BT, UK*
[b] *ISIS Facility, Rutherford Appleton Laboratory, Chilton, Didcot OX11 0QX, UK*

Received 29 October 2006; received in revised form 17 January 2007; accepted 18 January 2007
Available online 30 January 2007

Abstract

Neutron diffraction studies on hydrogen chemisorbed into the stage-1 graphite intercalation compound KC_8 are presented, including time-resolved scans across the hydriding transition to the saturated compound $KC_8H_{0.67}$. This transition involved a hydrogen-driven structural change taking place over 11.5 h. The Rietveld-refined structure of KC_8 was confirmed to be *Fdd*2 using GSAS. Proposed structures for the stage-2 saturated compound were fitted, the most successful being a tri-layer *C*12/*m*1 structure with a reduced χ^2 value of 1.940. A partial resolution of the in-plane structure is thus achieved, but further refinement is required to elucidate the hydrogen siting and the diffusion process.
© 2007 Elsevier B.V. All rights reserved.

Keywords: Hydrogen-absorbing materials; Neutron diffraction; Phase transitions

1. Introduction

Graphite intercalation compounds (GICs) formed by the insertion of alkali metals into the interlayer galleries of graphite are synthetic metals, renowned for their anisotropic physical properties [1,2]. These include examples of superconductivity, and the homogeneously stoichiometric long-range ordering known as staging, where stage-*n* denotes a compound with *n* graphite layers between each layer of intercalant metal. These are 'donor' GICs, because the interposed metal species relinquishes charge to the graphene sheets, creating a favourable charge environment for a second intercalated species in the augmented galleries. Of the possible ternary compounds, those with hydrogen as the third component are noteworthy both for their example as systems in which to study confined H_2 and their potential importance in energy storage research.

Two regimes exist for hydrogen uptake in alkali metal GICs, dependent principally on temperature [2]. Below 200 K is physisorption, where molecular hydrogen sites itself in local energy minima in the inter-graphene crystal field and is bound relatively weakly. Above 200 K the H_2 dissociates and binds chemically with the metal. This is known as chemisorption. Physisorption is easily reversible, and so it has been the focus of research into GICs as a means to store hydrogen. In the first-stage potassium-graphite compound KC_8, negligible physisorption is observed, while the second-stage analogue KC_{24} takes in up to 2.1 H_2 molecules per K ion below 100 K and at ambient pressure [2]. The notable difference between these two, apart from the alternating empty galleries in KC_{24}, is that the density of each metal layer is 3/2 greater in KC_8.This suggests a structural hindrance to the hydrogen uptake, which is not thought to enter empty layers.

Hydrogen is known to be chemisorbed by KC_8 at ambient temperature and above [3], giving compounds KC_8H_x up to a saturated value of $x = 0.67$. At 473 K this saturation is achieved at 133 mbar. A linear increase characterises *H* uptake for $0 < x < 0.1$, with a strong increase in sorption for $0.1 < x < 0.6$ and a levelling off to saturation above that. Characteristic of this process is a remarkable structural change of the compound from stage-1 to stage-2, as a result of potassium being entirely removed from alternate intercalated layers and combining with the dissociated hydrogen in remaining filled layers to form a triple layer of atomic planes, with a resulting *c*-axis sequence C-C-K-H-K-C, with the potassium electropositively and the hydrogen negatively charged. X-ray (0 0 l) diffraction analysis [4] gives the $KC_8H_{0.67}$ repeat distance as 11.88 Å, composed of

* Corresponding author. Tel.: +44 207 679 3409; fax: +44 207 679 7145.
E-mail address: arthur.lovell@ucl.ac.uk (A. Lovell).

0925-8388/$ – see front matter © 2007 Elsevier B.V. All rights reserved.
doi:10.1016/j.jallcom.2007.01.135

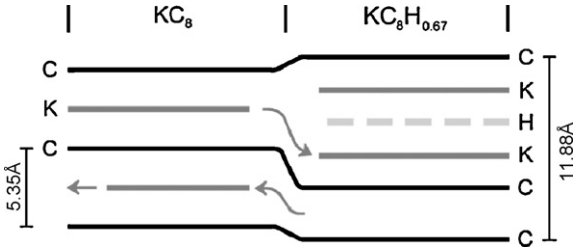

Fig. 1. Schematic showing hydrogen-driven conversion of stage-1 KC_8 to stage-2 KC_8 $H_{0.67}$ by domain-based phase exchange (after [4]).

an empty graphite layer 3.35 Å and an 8.53 Å filled layer thickness, fundamentally different from the 5.3 Å repeat distance of a K-filled layer in KC_8. For concentrations $0.1 < x < 0.6$ the two phases coexist, the sample undergoing a metal to non-metal transition with the ongoing hydriding sequence, until the 5.35 Å phase disappears entirely in favour of the stage-2 compound. A probable route for the transition mechanism is suggested as a domain-model (Fig. 1) though the driving factor is not clear but likely to be related to the dissociation enthalpy of the hydrogen.

Previous crystallographic studies [5] of the pristine KC_8 structure determined that it was orthorhombic, of space group *Fddd*, but Trewern et al. [6] found a better fit to the lower-symmetry *Fdd*2 with unit cell parameters $a = 4.92$ Å, $b = 8.59$ Å, and $c = 21.4$ Å. In the fully hydrogenated phase, a difference Patterson analysis placed the hydrogen midway between the potassium sheets. A 2×2 alternating potassium lattice structure was proposed, with hydride ions placed approximately in the tetrahedral vacancies between these layers. Three alternative models for the hydrogen-sorbed KC_8H_x structure were summarised by Miyajima et al. [7]: $a\left(2 \times \sqrt{3}\right)$ $R(0^\circ, 30^\circ)$, $a(2 \times 2)$ $R(0^\circ)$ and $a\left(2\sqrt{3} \times 5\right)$ $R(0^\circ, 30^\circ)$ hydrogen superlattice. But the stoichiometry of these, with $x = 0.5$, meant that more work was required to determine not only the correct structure but the in-layer siting of hydrogen ions for concentrations between 0.5 and 0.67.

This paper reports high-resolution neutron diffraction data on hydrogen introduced *in situ* into the interlayer spacings of KC_8 across a temperature range from 50 to 316 K, in a method intended to elucidate further the in-plane structure of the K–H interlayer hydride, to explore the physisorptive–chemisorptive regime boundary, and to chart the hydride transition with time-resolved diffraction.

2. Experimental

KC_8 was synthesised using a modified one-zone vapour transport process using 99.95% pure potassium (Sigma–Aldrich) and Papyex® exfoliated graphite strips. The graphite was outgassed under a 1.5×10^{-6} mbar vacuum at 773 K for several days before being placed in an argon glovebox. A 20% excess over the stoichiometric weight of potassium was inserted into a quartz tube with the graphite and this, sealed and evacuated, was placed in a furnace at 250 °C: the metal is melted onto the graphite strips inhomogeneously, then a 3-day annealing process results in well-staged samples with an even gold colour. The partially ordered exfoliated graphite was used for its preferential uptake of hydrogen and the relative facility of the intercalation process, compared with highly oriented pyrolytic graphite (HOPG). It demonstrates a strong preferred orientation, which had to be accounted for in the experimental setup.

Neutron diffraction was carried out on the POLARIS high-resolution diffractometer at ISIS. 0.3557 g of KC_8 was placed in a flat Ti–Zr cell and placed into the POLARIS cryostat. Angular variation of the sample was used to distinguish between the in-plane and out-of-plane scattering in the optimised detector banks. Data were collected on KC_8 at 50 K with the preferred orientation *c*-axis aligned at 45° and 90° to the incoming beam, before exposure *in situ* to 99.999% pure pre-cryopumped hydrogen gas. No structural change was observed on hydrogen loading, so a 3×10^5 Pa pressure of hydrogen was put on the sample and the temperature raised to trace any physisorption and find the minimum temperature of the transition, with measurements at 50, 100, 150, and 200 K showing no structural changes in the compound. The staging transition was observed to begin at 250 K but its rate was very low so the temperature was raised further. The largest transition rate was measured between 300 and 314 K and the sample was fully stable in the new phase after 11.5 h for a final temperature of 316 K. Data were collected at c-axis orientations of 90° and 45° to the incident beam on $KC_8H_{0.67}$. Short time-resolved data runs were taken over the transition. Pumping to a vacuum of order 10^{-6} mbar and cooling the sample to 250 K was not seen to remove hydrogen; thus the transition appears irreversible within the limits of the timescale and temperature environment available.

3. Results

The minimum temperature for the phase change, and hence the critical temperature for the physisorptive-to-chemisorptive transition at this pressure, was found to be 250 K, though the hydrogen overpressure reduced very slightly from 2.940 to 2.938 bar between 210 and 250 K. Analysis of the phase change shows a two-stage process. First, a broadening of the KC_8 peaks without significant structural change, incorporating a reduction in peak intensity. Second, an augmentation of the lattice parameter is followed by the progressive generation of the new phase and extinction of the first. Following [8], this provides evidence for hydrogen dissociation in interstitial sites in the layers as a forerunner to the charge transfer from KC_8 to H and the structural transition.

Data were collected in all available detector banks; initial characterisation of the 90° oriented sample was done utilising low-angle scattering to align the scattering vector, *Q*, as closely as possible to the preferred orientation axis. This enabled characterisation of the (0 0 l) peaks as the transition occurred, the clearest signature of the completed transition being the disappearance of the KC_8 out of plane scattering in favour of that of $KC_8H_{0.67}$. Fig. 2 samples the diffraction data as a function of the elapsed time of the transition. The (0 0 4) and (0 0 8) peaks of KC_8 at 5.35 and 2.66 Å, respectively reduce, diminishing rapidly after two hours as (0 0 l) peaks of the hydrogen-saturated $KC_8H_{0.67}$ phase grow at 2.98 and 3.95 Å. The characterisation of these peaks depends on the stacking structure of the $KC_8H_{0.67}$ phase; for the simplest structure with 11.88 Å *c*-axis parameter, these are the (0 0 4) and (0 0 3) peaks, respectively. The total transition time observed is considerably shorter than reported elsewhere [7,9,10], which may be characteristic of the kinetic effect of the higher pressure of hydrogen. A transition time of 18 h was reported in [6] for an exfoliated graphite sample similar to that used in the present case; however, the partially oriented nature of the crystallites in exfoliated graphite improves the sorption and transition kinetics.

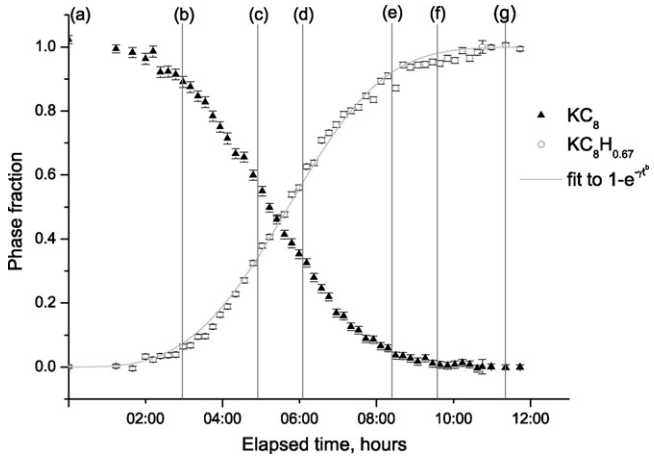

Fig. 2. Phase fractions of KC_8 and $KC_8H_{0.67}$ over the phase transition. The letters refer to the time-resolved diffraction patterns in Fig. 3.

Fig. 2 shows the phase fractions by integrated peak intensity of the two phases as a function of the elapsed time of the transition. It is not certain whether the rate-limiting factor on the transition is the absorption at the crystallite edges or diffusion of the hydrogen through the bulk material. From the relative rapidity of the transition in the exfoliated sample, either might be deduced, though an attempt to fit a function of the form $1 - e^{-(2/3)\gamma t^{3/2}}$ to the time-dependent growth of the hydrogenated phase, based on the diffusion of hydrogen into the sample, was not successful: a fit of the form $1 - e^{-\gamma t^b}$ is shown in Fig. 2, where $\gamma = 86.25 \pm 7.72$ and $b = 3.36 \pm 0.07$. If compared to an Avrami model the time power, b, suggests the new phase nucleates in a manner between two and three-dimensional ($3 > b > 4$), characteristic perhaps of a planar solid such as KC_8, though as the process is not isothermal this cannot be confirmed with the present data. Fig. 3 shows the transition through the diffraction, with time-ordered diffraction patterns.

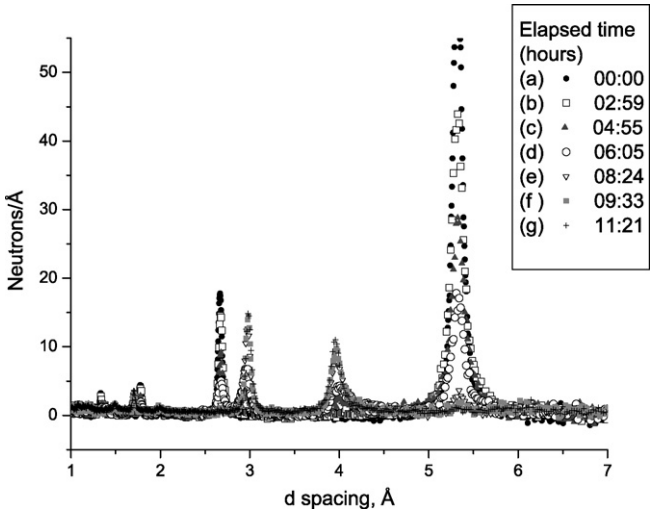

Fig. 3. Time-resolved c-axis diffraction patterns from the transition period marked with the time elapsed since the beginning of the transition.

4. Data fitting and discussion

The diffraction data were analysed using Rietveld methods. Data fitting was performed using the GSAS package [11], incorporating the EXPGUI interface [12]. The optimum fitting was performed on data from the 45° c-axis sample orientation from neutrons scattered into the 90° detector banks, which were decoupled so that left and right banks summed independently. With this configuration, the scattering vector Q for these banks lay parallel to the c-axis on the right side of the instrument, as seen facing the neutron source; hence within the variation given by the mosaic spread of the graphite, all the scattering was out-of-plane in the right-side 90° detectors. On the left side Q lay perpendicular to the c-axis, hence there was predominantly in-plane scattering recorded in the left side 90° detectors. Separate fits were made for the in-plane and out-of-plane scattering. Preferred-orientation analysis was carried out by refining the data to a March–Dollase function [13] within EXPGUI. Background measurements run on an identi-

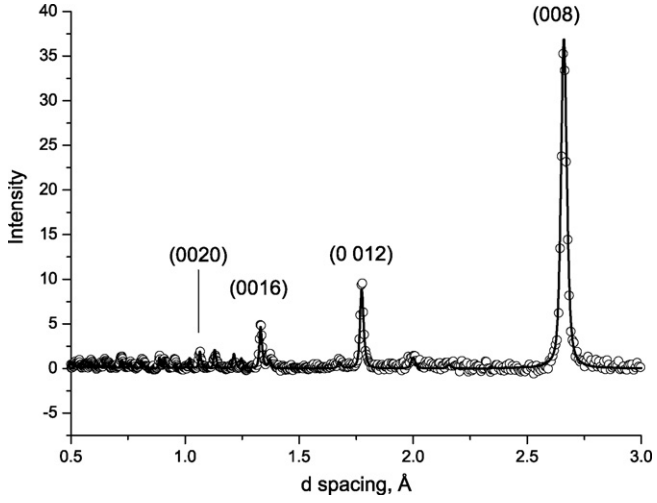

Fig. 4. c-Axis scattering from KC_8 with GSAS fit.

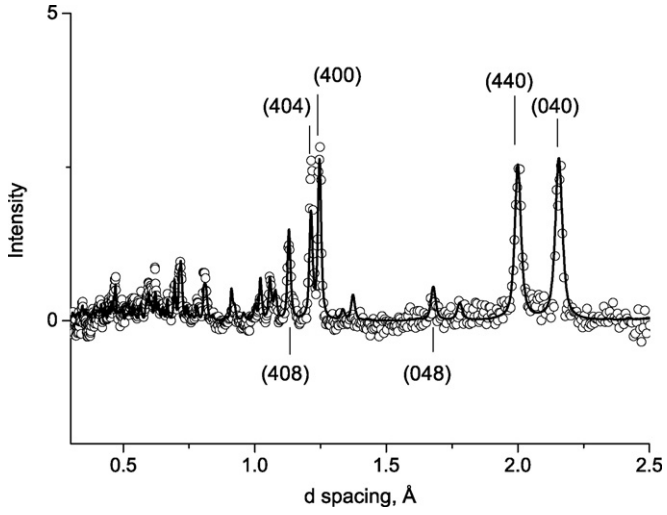

Fig. 5. KC_8 in-plane scattering, with GSAS fit.

Table 1
Proposed structures for KC_8H_x and the fitted χ^2 values to the data

Structure name	*H* superlattice	Graphene layer stacking	Space group	Best fit χ^2
KC_8H_1 1 layer	$1 \times \sqrt{3}R(0°, 30°)$	AAA	*Cmma*	3.503
KC_8H_1 2 layer	$1 \times \sqrt{3}R(0°, 30°)$	AABBA	*Cmca*	2.375
KC_8H_1 3 layer	$1 \times \sqrt{3}R(0°, 30°)$	AABBCCA	*C*12/*m*1	1.940
$KC_8H_{0.5}$ 1 layer	$2 \times \sqrt{3}R(0°, 30°)$	AAA	*Pccm*	9.096
$KC_8H_{0.5}$ 2 layer	$2 \times \sqrt{3}R(0°, 30°)$	AABBA	*Pcca*	6.198
$KC_8H_{0.5}$ 3 layer	$2 \times \sqrt{3}R(0°, 30°)$	AABBCCA	*P*12/*c*1	–
$KC_8H_{0.5}$ 1 layer hexagonal	$2 \times 2R(0°)$	AAA	*C*222	3.153
$KC_8H_{0.5}$ 2 layer hexagonal	$2 \times 2R(0°)$	AABBA	*C*2221	2.763
$KC_8H_{0.5}$ 3 layer hexagonal	$2 \times 2R(0°)$	AABBCCA	*C*121	2.061

cal sample cell setup showed a quasi-continuum of scattering without Bragg peaks, due to the null-coherent-scattering Ti–Zr cell and Cd shielding. This allowed the background to be fitted to an 8-variable Chebyschev function and subtracted within the fit.

Results of the fit for the initial KC_8 sample confirmed an *Fdd*2 orthorhombic structure with lattice parameters $a = 4.965$ Å, $b = 8.628$ Å, and $c = 21.249$ Å. The fitted out-of-plane pattern is shown in Fig. 4. As in previous studies, the in-plane scattering, shown in Fig. 5, was harder to refine; in particular, certain peak intensities are fitted less successfully, such as the (4 0 4) reflection at 1.209 Å and the (8 0 0) at 0.621 Å. The overall reduced-χ^2 for the fit was 1.419 for 10 variables.

Fitting the saturated $KC_8H_{0.67}$ sample proved more difficult due to the lack of a completely resolved in-plane structure. Proposed structures in the literature have assumed a single-layer graphite stacking, such that graphene sheets in adjoining layers can always be superposed in the *c*-direction. This is based on the graphite stacking in KC_8, which is characteristically AAA as the intercalated K ions lock the planes congruently. There is no such constraint on the empty galleries in $KC_8H_{0.67}$; however, by analogy with the second-stage compound KC_{24} or pristine graphite [1] there could be graphite stacking AABBA or AABBCCA; the hydride intercalated layers lie between like planes with the C-K-H-K-C layer unit above translated by the length of a carbon–carbon bond over the empty gallery. Expanding the proposed structures to incorporate this possibility reduces their symmetry and hence increases the fitting calculations. A list of the structures fitted appears in Table 1 together with the optimum fit χ^2-values found for each. The best-fitted structure of these is the tri-layer KC_8H_1, with space group *C*12/*m*1 and lattice parameters $a = 4.949$ Å, $b = 8.577$ Å, $c = 38.303$ Å, angles $\alpha = 90.0°$, $\beta = 105.1°$, $\gamma = 90.0°$. Fits of this structure to the *c*-axis and in-plane scattering are shown in Figs. 6 and 7. The fits are good at low *d*-spacing but have several deficiencies. The stoichiometry of KC_8H_1 is incorrect for the saturated sample but sample structures with 0.67 H per K were too low symmetry to fit. Instead, attempts to fit the hydrogen occupation number for this structure were made but were inconclusive. The partial success of the fit qualitatively backs up the proposals for the in-plane K structure, which are unchanged across all models, but suggests more investigation and modelling could profitably be carried out to elucidate the in-plane hydrogen structure.

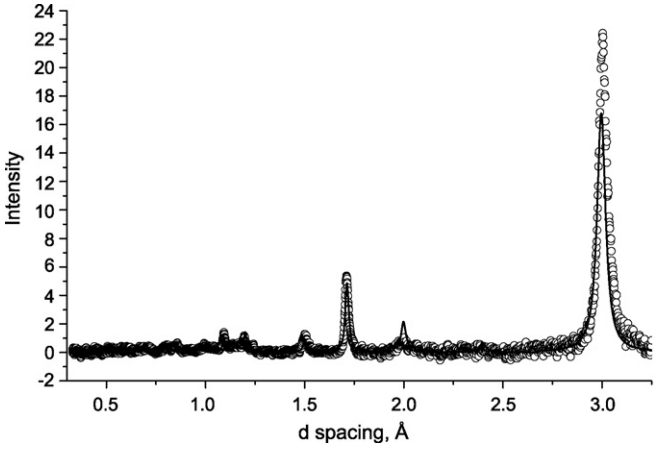

Fig. 6. *c*-Axis scattering from $KC_8H_{0.67}$ with GSAS fit.

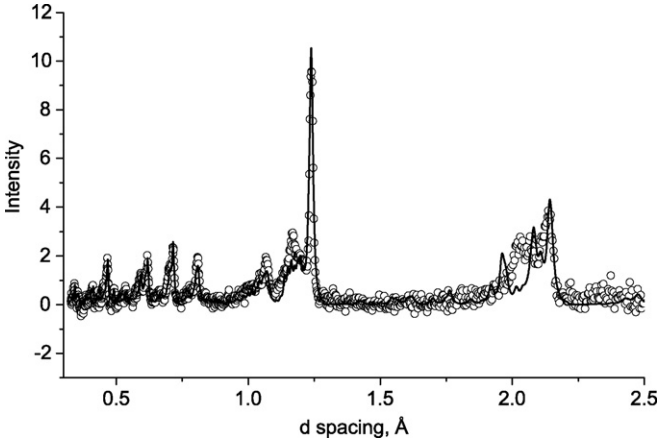

Fig. 7. $KC_8H_{0.67}$ in-plane scattering with GSAS fit.

5. Conclusions

This study has provided high-resolution time-resolved neutron diffraction data for the hydrogen-driven transition in KC_8H_x using a 3×10^5 Pa overpressure of hydrogen gas and raising the sample temperature from 50 K *in situ*. The onset of the transition was found to occur at 250 K with some uncertainty due to the very slow initial rate of the second phase formation. The transition was accelerated co-incident with a further raise in temperature to a maximum of 316 K: the maximum rate of the phase transition occurred from 300 K. This gave a total transition

time of 11.5 h, significantly less than reported elsewhere under lower hydrogen pressures and in more highly oriented graphites. Structural fitting based on Rietveld refinement of the KC_8 phase confirmed an *Fdd*2 structure. Fitting possible structures to the hydrogen-saturated $KC_8H_{0.67}$ phase suggested a tri-layer unit cell with stacking graphene stacking A|AB|BC|CA, where | are K-H-K intercalated hydride layers. The best fit was obtained for a structure of KC_8H_1 with a $1 \times \sqrt{3}R(0^\circ, 30^\circ)$ hydrogen superlattice. It is not certain if the stoichiometrically exact structure of $KC_8H_{0.67}$ can be expressed as this structure with 1/3 hydrogen vacancies on present evidence. These models improve understanding but are not adequate to fully define the in-plane hydrogen structure and thus further refinement is necessary.

Acknowledgment

The authors wish to thank Dr. A.H. Harker (UCL) for discussions regarding phase growth modelling.

References

[1] M.S. Dresselhaus, G. Dresselhaus, Adv. Phys. 51 (2002) 1–186.
[2] S.A. Solin, H. Zabel, Adv. Phys. 37 (1988) 87–254.
[3] D. Saehr, A. Hérold, Bull. Soc. Chim. Fr. (1965) 3130.
[4] M. Colin, A. Hérold, Bull. Soc. Chim. Fr. (1971) 1982.
[5] P. Lagrange, D. Guerard, A. Hérold, Ann. Chim. E 3 (1978) 143.
[6] T. Trewern, R.K. Thomas, G. Naylor, J.W. White, J. Chem. Soc., Faraday Trans. I 78 (1982) 2369–2385.
[7] S. Miyajima, T. Chiba, T. Enoki, H. Inokuchi, M. Sano, Phys. Rev. B 37 (1988) 3246.
[8] T. Enoki, M. Sano, H. Inokuchi, J. Chem. Phys. 78 (1983) 2017.
[9] T. Enoki, M. Sano, H. Inokuchi, Phys. Rev. B 32 (1985) 2497.
[10] S. Miyajima, M. Kabasawa, T. Chiba, T. Enoki, Y. Maruyama, H. Inokuchi, Phys. Rev. Lett. 64 (1990) 319.
[11] A.C. Larson, R.B. Von Dreele, General Structure Analysis System (GSAS), Los Alamos Nat. Lab. Report LAUR 86-748, 2004.
[12] B.H. Toby, J. Appl. Cryst. 34 (2001) 210–221.
[13] W.A. Dollase, J. Appl. Cryst. 19 (1986) 267–272.